THE 10-GEV SYNCHROTRON AT CORNELL

A new electron accelerator, to be dedicated this month, continues the tradition at Cornell University. Elementary-particle research, including tests of quantum electrodynamics in electromagnetic interactions and studies of the vector-meson family, will benefit.

BOYCE D. MCDANIEL and ALBERT SILVERMAN

On 10 October Cornell University and the National Science Foundation will join in the dedication of the Wilson Synchrotron Laboratory and its associated facilities. This laboratory houses the 10-GeV electron synchrotron, the fourth in a series of electron accelerators built and used by physicists at Cornell under the inspiration and leadership of Robert R. Wilson for whom the new laboratory is named. The new machine was conceived in August 1962; in March 1965, after two and a half years of design study and finance negotiations, a construction contract was signed. Two years later a beam circulated in the machine and in March 1968 we obtained full energy of 10 GeV. This is the highest energy yet attained in any electron synchrotron. The experimental-physics program utilizing the accelerator started in November 1967, at which time the synchrotron was already operating at an energy of 7 GeV.

Budget, scale and site

The total construction budget, including machine and laboratory, amounted to about 12 million dollars. After an increase in the scope of the project somewhat beyond that of the original plan, construction was completed for less than the budget figure in a time shorter by many months than the three and a half years' contract time.

A "preoperating" budget of $650 000 helped us prepare for the experimental program. With the start of experiments we had a further 2.2 million dollars to support the first year of operation and the experimental program, including the purchase of further capital equipment. With these allocations we have equipped the first round of experiments, although the total amount of equipment available, such as magnets, spectrometers and so on, is still very limited.

The accelerator,[1] a strong focussing device, has a magnetic guide field with a perimeter of about 0.8 km. Its tunnel, dug out with a boring machine, lies 14 meters under an athletic field near the center of the Cornell University campus at Ithaca. This remarkable site was chosen so that the research activities could be closely coupled with the interests of the whole academic community and, in particular, with the activities of the department of physics. The synchrotron ring passes through the experimental hall and extends back under the field in the circular tunnel of 3-meters diameter (see figures 1 and 2).

The machine provides a beam at energies up to 10 GeV with an intensity of 3×10^{10} electrons per pulse at 60 cycles per second. We hope to increase the intensity to about 10^{11} electrons per pulse soon. So far none of our experiments has been limited by lack of intensity.

We have found the accelerator an

Albert Silverman came to Cornell in 1950 with bachelor's and doctor's degrees from Berkeley. Fulbright, Guggenheim and Ford Foundation fellowships took him to Frascati, where he worked on polarization of the recoil proton in π^0 photoproduction, and to CERN, where he studied proton-proton scattering at high energies and large angles. Now at Cornell his research includes meson photoproduction and Compton scattering from hydrogen.

Boyce D. McDaniel, director of Cornell's Laboratory of Nuclear Studies, took his PhD at Cornell after obtaining bachelor's and master's degrees at Ohio Weslyan University and the Case School of Applied Science. He worked in Canberra and Frascati under Fulbright and Guggenheim Fellowships, and has been a member of the Cornell faculty since 1946. His research has been in slow-neutron and gamma-ray spectroscopy, and k-meson photoproduction.

CUTAWAY VIEW OF THE CORNELL SYNCHROTRON shows the tunnel 13 meters below the athletic field. The straight tunnel across the diameter is for utilities and is also an escape route to the surface. Laboratory building is above ground level in scenic Cascadilla Gorge. —FIG. 1

exceptionally satisfying instrument. It is very reliable and those difficulties that have occurred are reasonable and understandable; most have been of the sort that will be eliminated during the first year of "wearing-in" the machine. Our performance record in the last six months of running shows that an acceptable beam is provided by the machine for more than 85% of the scheduled hours, which are 16 eight-hour shifts each week.

Personnel and methods

Nearly all those who were engaged in the major technical aspects of the design and construction of the accelerator were physicists simultaneously involved in teaching and research. Four of our professorial staff were involved in a major way, and an equal number in part-time fashion. Three research associates put their full time to the project. Nearly all of those physicists involved had previously taken some major responsibility with at least one of the earlier Cornell synchrotrons. We could boast of only three engineers on our staff.

The average number of employees involved during the construction was about 35, not including the physicists. Now that the machine is functioning we employ about 25 persons who operate and maintain the facility and assist in setting up experimental apparatus. Another 20 persons are connected with various service facilities such as stock room, business office and central shop facilities.

We set up our own assembly line for the construction of the magnets and the supporting modules; nearly all the components of the injection system were constructed in our own shops, and we made the entire power-supply equipment for the excitation ourselves. For the multiplex control only the mass production of transistor cards was done outside.

THE ACCELERATOR

The basic lattice of the machine has six sectors, each made up of 32 magnets in the pattern: radial focus-defocus-defocus-focus. The field gradient chosen for the machine is such that the vertical and radial betatron-oscillation frequencies are each 10.75 times the orbital frequency. The lattice incorporates four 6.1-meter straight sections and two diametrically located 12.2-meter straight sections. The 6.1-meter field-free regions accommodate the accelerating cavities, and the longer ones provide ready access to the circulating electron beam for internal targets and other devices. To minimize loss of aperture, owing to these field-free spaces, Collins-type insertions[2] were made. In the 6.1-meter sections the two magnets nearest the straight sections have a special strong-

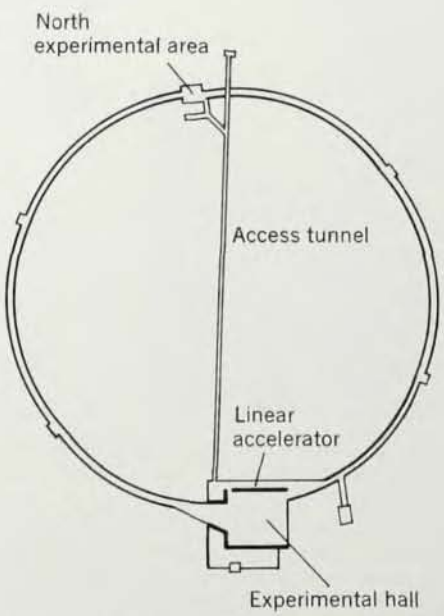

PLAN OF SYNCHROTRON and experimental hall. Radiofrequency accelerating cavities are in the four small rooms on the tunnel perimeter. —FIG. 2

Synchrotron Parameters

Electron energy	10 GeV
Radius of curvature in magnet	100 meters
Repetition rate	60 Hz
Nominal intensity	10^{11} electrons/pulse
Number of magnet units	192
Long straight sections	2 of 12.2-meter length 4 of 6.1-meter length
Gap height, focus and defocus respectively	2.54 and 3.80 cm
Gap width, good field	5.5 cm
Magnetic field at 10 GeV	3.3 kG
Betatron oscillations/turn $\nu_V = \nu_R$	10.75
Linac energy	150 MeV
Linac frequency	2855 MHz
rf frequency	714 MHz
rf voltage/turn at 10 GeV	10.5 MeV

ELECTRON SYNCHROTRONS

The basic elements of a synchrotron are the injector, guide field and accelerating device. A linear accelerator introduces electrons into a closed magnetic guide field with a strength that increases with time. At injection time the magnetic field is matched to the momentum of the injected electrons to produce the correct orbit radius. The electrons are accelerated by radiofrequency cavities; the principle of phase stability keeps the electron momentum matched to the increasing magnetic field. The electrons always have a velocity very near that of light, so that for a constant orbital frequency the orbit radius is constant. The peak energy is achieved at the maximal value of the magnetic field.

The Cornell synchrotron has a peak operating energy of 10 GeV; the maximum energy is 7 GeV for other currently operating electron synchrotrons in the world. The synchrotrons that now operate at 5–7 GeV are NINA, Daresbury, England; DESY, Hamburg, Germany; Eravan, USSR and CEA, Cambridge, Mass. The Cornell machine accelerates 3×10^{10} electrons per pulse at 60 cycles per second. The intensity is expected to exceed 10^{11} per pulse in the near future. This flux is comparable to that provided by the other synchrotrons.

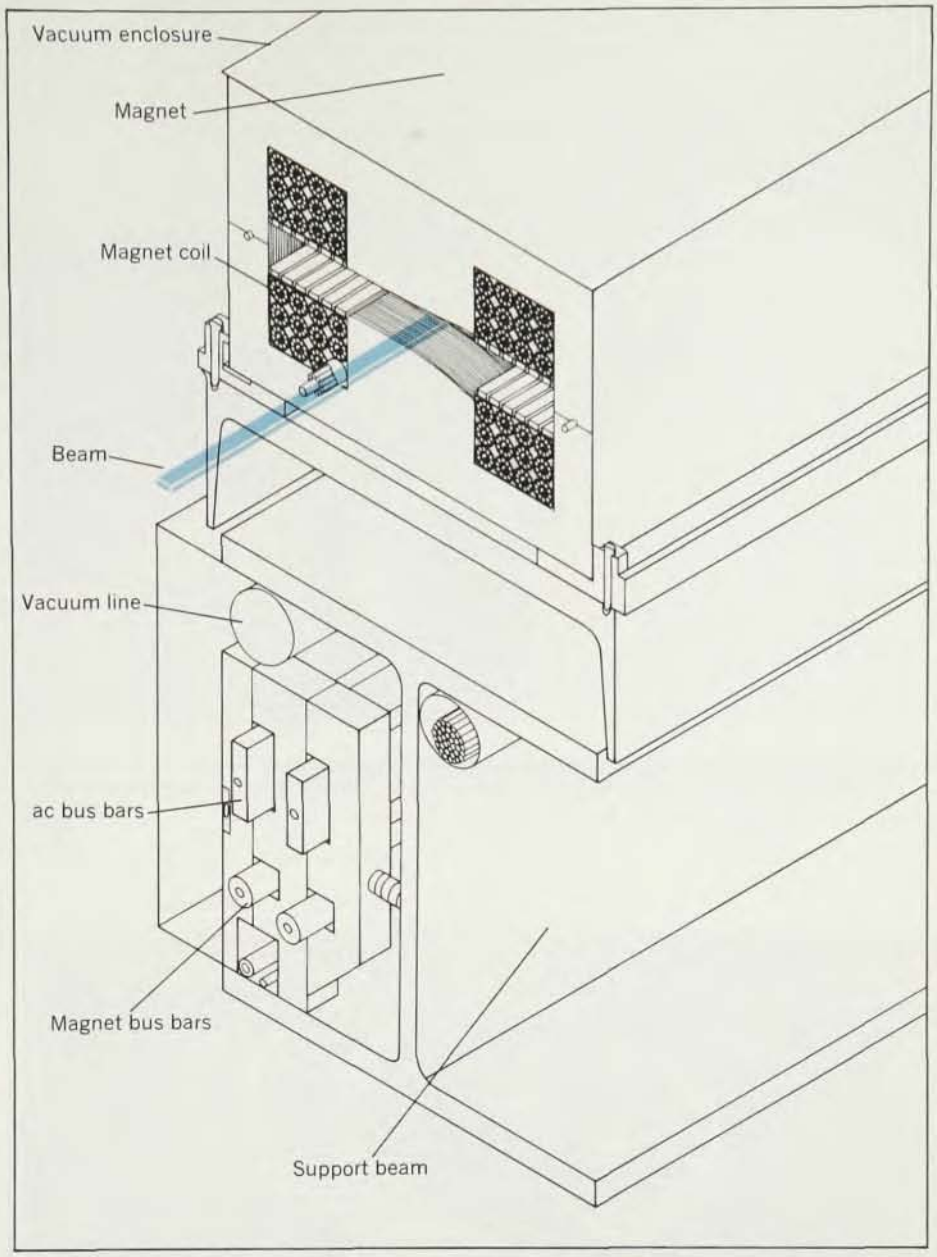

CROSS-SECTION OF MAGNET showing position of electron beam (color). Entire magnet is enclosed in vacuum chamber; power circuits and vacuum lines are enclosed between the webs of the I-beam support beneath the magnet. —FIG. 3

gradient profile that leaves the entire space unencumbered, but in the 12.2-meter sections we use a quadrupole pair to provide the proper insertion. These quadrupoles, each about 76 cm long, are about 30 cm apart and are located symmetrically about the midpoint of the straight section. The total amount of material obstructing the vicinity of the median plane of the magnet is a minimum, so that we have the greatest flexibility for emergent beams from these straight sections.

Electrons are given their initial injection energy by a 150-MeV Varian S-band linear accelerator, located inside the ring, and after suitable momentum analysis they enter the synchrotron guide field. The specifications for the linear accelerator are such that 100 milliamps of electrons fall in a one-percent momentum interval. The pulse duration is 2.5 microseconds, the filling time for single-turn injection into the ring.

Small guide-field magnets

The 192 magnets that make up the guide field are of novel design, with design features, determined by a number of related considerations, that keep them unusually small. The radiofrequency voltage required to make up for the synchrotron-radiation loss is proportional to E^4/R where E is electron energy and R is radius. Thus the rf power that is required rises very rapidly as the electron energy is increased. There are two advantages of a large radius; the required voltage per turn decreases as $1/R$, so the power decreases as $1/R^2$, and more space is available in the straight sections for accelerating cavities. The total radiofrequency power for the same accelerating voltage decreases inversely as the length of the cavities. The net effect of these two factors (radius and cavity length) is to make the required power decrease approximately inversely as the cube of the radius of the machine. For these reasons the radius of the ring was chosen so great—the instantaneous bending radius in the magnets is 100 meters. Though it might seem that the additional length would significantly increase the cost of the magnet, this is not so; the required field strength for 10 GeV is only 3300 gauss, with a great relative saving in iron and copper and in magnet power.

Figure 3 shows a cross section of a guide-field magnet. Each one is approximately 3.4 meters long, built of

INTERIOR OF THE SYNCHROTRON TUNNEL. Magnets are inside the rectangular vacuum chamber on top of the support beams, and capacitors and biasing choke transformers are mounted under the beams. Tunnel diameter is 3 meters. —FIG. 4

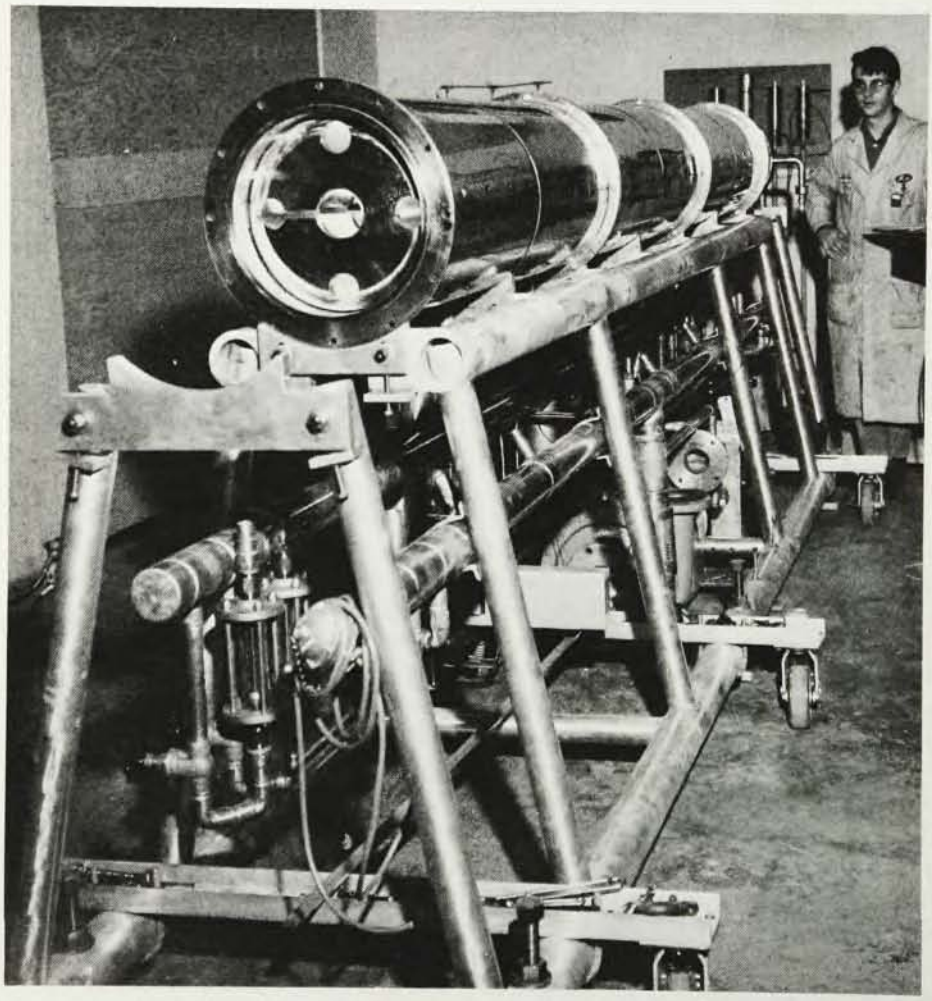

RADIOFREQUENCY ACCELERATING CAVITY shows diaphragm with keyhole slot in median plane. Four holes at larger radius provide coupling between successive elements of the structure. External diameter of cavity is 33 cm. —FIG. 5

laminations of 29-gauge Armco A6 high-silicon steel. Each lamination profile is that of an H bisected in the median plane. The outside dimensions of each magnet are only 20.3 × 29.2 cm, with gaps of 2.5 and 3.8 cm at the central orbit for the radially focussing and radially defocussing lenses respectively. This variation of gap height between the two types of lenses involves no loss in useful aperture because the vertical betatron oscillations are confined in an undulating envelope with maxima occurring within the radially defocussing lenses only.

We computed the proper profile for the required gradient by conventional methods and constructed a sample magnet with the appropriate two-stage die to verify the design and determine the useful range of the radial aperture; then we went into the full-scale stamping process. A total of 4 million laminations, weighing approximately 200 tons (180 000 kg), were shuffled thoroughly to minimize orbit distortions arising from nonuniformities in the iron.

We fabricated the magnet on site by stacking the laminations on a jig, upper and lower half separately. Prefabricated excitation coils were laid in the window space of the stacked laminations and bonded in place with epoxy. Narrow lead strips, epoxied on the face of the coil toward the median plane, provided protection for the coils against radiation damage from the synchrotron radiation and injected electron beam. After curing the epoxy we keyed the upper and lower sections of the magnet by glass dowels and epoxied them together. As a final operation the whole magnet was slipped into a 0.8-mm stainless-steel jacket and sealed by arc welding.

Extensive magnetic measurements on each magnet included gradient, residual field, eddy-current effects, high-field flux, saturation characteristics and the location of the isomagnetic line. Because of fringe-field effects we took special care to provide the correct contour of the pole at the ends of the magnet. This profile was manufactured from normal laminations by shearing individual laminations in a progressive pattern. Figure 4 shows the magnets assembled on their support structure in the tunnel.

Two stages of alignment

To obtain and preserve the required high accuracy in alignment we de-

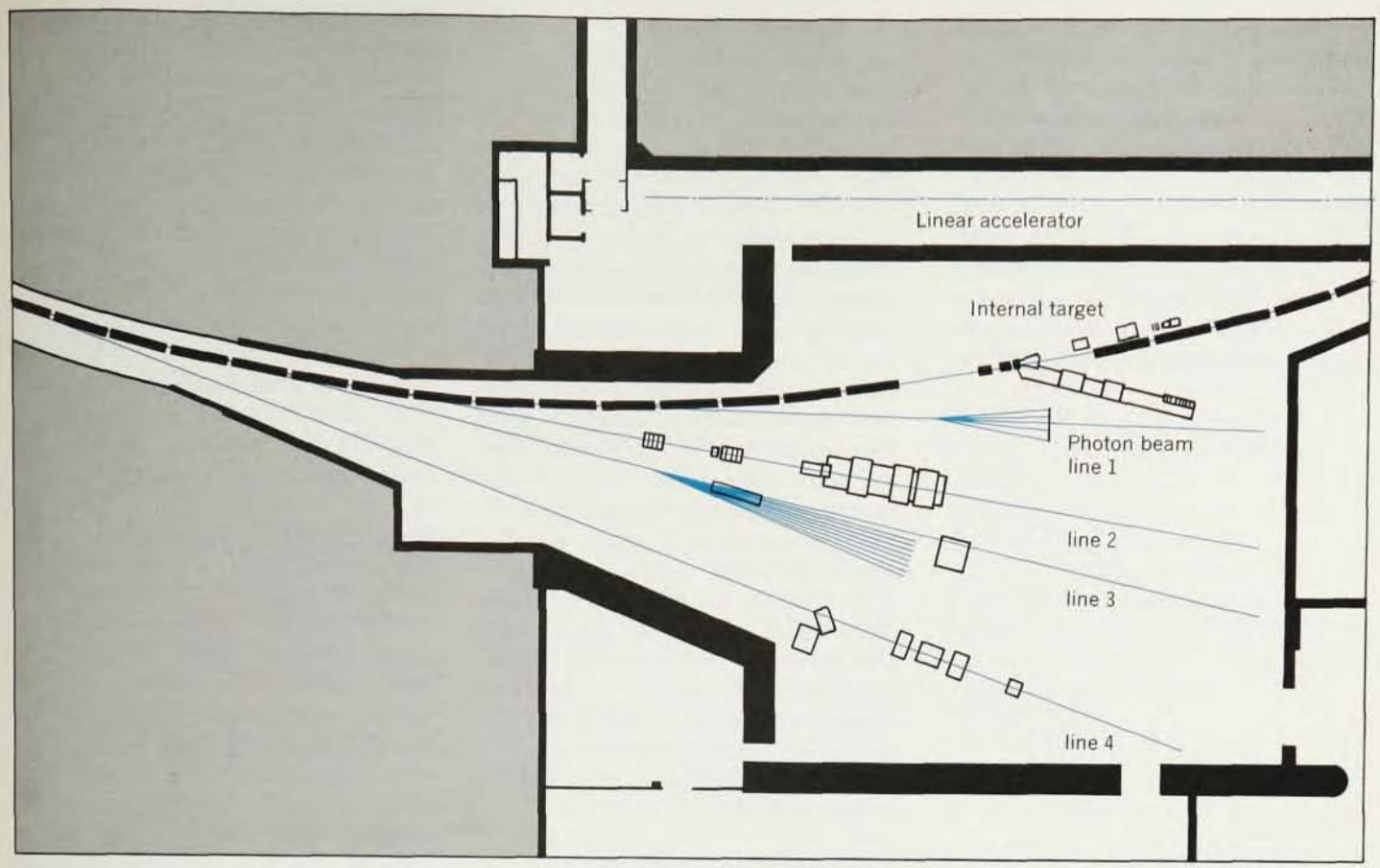

WEST FLARE AND EXPERIMENTAL HALL. Linear-accelerator injector is on center line shown; beam paths are in color. Beam lines currently in use are the internal-target bremsstrahlung experiment and the four photon beams. All are shown in greater detail in later figures. —FIG. 6

cided, rather than have piles driven far below the tunnel for a rock-steady support, to provide adjustment jacks directly on the concrete floor of the tunnel and make regular checks of alignment accuracy.

Alignment of the machine was then accomplished in two stages. First, a careful conventional optical survey utilized 48 simple demountable piers mounted to the walls of the tunnel. This survey, on the initial transit, closed to about 1.2 cm, and a resurvey then checked alignment after smooth distribution of the error. Using this coarse grid, we laid sections of the guide field, approximately 60 meters long, in place. Special fixtures mounted on top of each of the magnets, together with stretched wires and suitable jigs, provided precise offsets between magnets so that the position of one magnet relative to its immediate neighbors could be determined with high precision. The stretched-wire technique yielded alignments better than 0.02 mm, but because of other problems the relative alignment of nearby magnets is probably good to only 0.1 mm. We believe that the final alignment is such that the magnets conform to the proper path with an ellipticity not exceeding 0.7 cm, and over a betatron wavelength, 70 meters, the accuracy of alignment is believed to be of the order of 0.04 cm. We have encountered no difficulty that could be ascribed to bad alignment of magnets; however, orbit deviations of the order of 1.0 cm are observed in certain locations. We believe these deviations are explained either by survey errors or failure to take into account known deviations of the isomagnetic lines for individual magnets. To simplify the alignment these latter deviations were ignored.

Magnet power and cavity design

In the magnet-excitation circuit the magnet inductance is tuned with capacity so that it is series resonant at 60 Hz. The resonating capacitors are distributed between adjacent magnets of the guide-field ring, with the advantage that no large accumulation of ac voltage arises between any point of the magnet circuit and ground potential.

To minimize total ac losses, a positive dc bias applied to the sinusoidal magnet current eliminates its wasted negative excursion. The dc bias is then approximately half of the peak-to-peak ac current.

Total power requirement for operation at 10 GeV is 770 kilowatts, of which 410 kW of ac excitation is supplied by a solid-state inverter.

To compensate for errors in the magnet guide field at injection time there are 40 sets of small vertical and horizontal correction coils at intervals of approximately one quarter of a betatron wavelength. The errors that these coils correct arise from inhomogeneities in the iron, magnet-fabrication variation, survey errors and parasitic magnetic-excitation currents. The currents in the correction coils are dc and are digitally controlled in 60 intervals. There is a similar set of 12 quadrupole-gradient corrections.

Four cavity structures similar to that shown in figure 5 provide the acceleration of injected electrons; each structure is a waveguide consisting of 15 perforated diaphragms mounted in a cylindrical tube. Each cavity is coupled to a klystron power tube op-

erating at 714 MHz, the fourth submultiple of the linear-accelerator frequency, and the power tubes are driven by a centrally located plate-modulated klystron driver. The cavities operate in the traveling-wave mode.

The external diameter of the cavity is 33 cm, and its length is 4.9 meters including the couplers at each end of the assembly; thus the 6.1-meter straight sections are nearly filled by the cavity structure. The hole in the waveguide diaphragm is 7.6 cm in diameter and provides full aperture for the beam. A special slit, extending radially outward in the median plane from the central hole in the diaphragm, reduces the possibility of "multipactoring" in the cavity, that is, a vacuum discharge caused by regenerative secondary emission of electrons from the cavity walls, induced in this case by synchrotron radiation. An experimental model without such a keyhole slot had serious problems when tested in our 2-GeV accelerator. Keyhole slots in the median plane prevent photoelectrons from being released in the high electric-field region near the axis of the cavity. In operation, each of the cavities has independent phase control, and we find the proper relative phases by experimentally adjusting them for acceleration of beam to maximal energy for a fixed power input. The average rf power requirement is 136 kW, and the peak rf power is 425 kW.

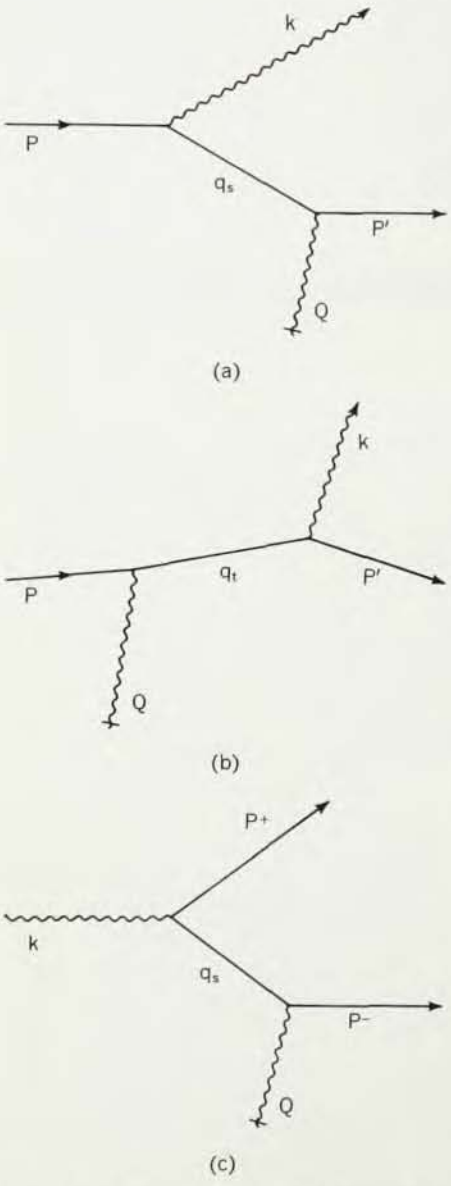

BREMSSTRAHLUNG (a and b) and pair production (c) shown in Feynman diagrams. q is the 4-momentum of the virtual lepton; it is space like, q_s, for pair production and either space like or time like in bremsstrahlung. Either q_t or q_s can be made small by a suitable choice of kinematic conditions. In the symmetric case (as in the experiments described in text) momentum given to nucleus is small; invariant mass of the final lepton pair is given by $m^2 \approx 2q^2$. —FIG. 7

Vacuum system

The arrangement of our vacuum chamber is another factor that helps to reduce the size of the magnets. There is no vacuum chamber in the magnetic gap; the entire magnet is evacuated by surrounding it with a thin, stainless-steel vacuum jacket so that no vertical aperture is sacrificed to provide the vacuum. As might be expected, all this material inside the vacuum system results initially in a poor vacuum. However, after a routine outgas at high temperature for about two weeks, a pressure of a few times 10^{-6} torr can be maintained. We have observed no significant increase in pressure in the operating synchrotron during full excitation and normal operation. All vacuum components of the machine are stainless steel, and the quick-disconnect vacuum flanges are designed for copper gaskets. There are 104 oil-diffusion pumps in the main synchrotron ring.

Computer control and monitoring

The beam intensity in the machine, as well as vertical and horizontal position of the circulating beam, is determined by ferrite-induction beam-detection devices. A ferrite loop, closed around the beam, monitors circulating electrons with a pick-up winding connected as a current transformer. Four bars of ferrite, forming a rectangle with short air gaps, constitute each unit for locating the position of the beam in the gap. Windings that pick up the flux induced by the beam provide a signal proportional to the displacement from the center of the rectangle, so enabling us to measure both vertical and horizontal displacements. There are 40 of these detectors distributed roughly one quarter of a betatron wavelength apart around the perimeter of the machine.

One of the unique features of our accelerator is the simplicity with which it is controlled and monitored. A time-sharing multiplex system addresses and monitors several functions at each of the 102 support tables for the main ring. Oscillographic displays present serially, on a single trace, the values of a chosen variable for each of the stations. These variables include amongst others vacuum pressure, magnet temperature, exciting current in the magnet that drives the transformer and voltage between the main winding and ground. As well as these continuous displays we can dial suitable addresses to apply control voltages that provide current for the low-field correction coils, survey jack motors to correct magnet alignment and relays for fast coaxial switches connected to the beam intensity and position monitors. The entire machine can be controlled from a single, compact, control desk by one operator.

An IBM 1800 computer helps to monitor and control the machine, although the accelerator will operate without it. The computer performs supplementary services for the operator, for example, recording in its memory the various control variables for the machine. If, after manual tuning of the machine, we want to restore an old set of parameters into the controls we can do it by reading the old values, from the computer memory, into the controls with motorized potentiometers. The computer also monitors and maintains various parameters within safe limits.

We can also use the computer to control the low-field correction coils automatically, in order to optimize the beam intensity. A localized orbit distortion can be applied at a given point of the guide field so that we can explore the aperture limits at that point by sensing the intensity of the accelerated beam. This distortion can be adjusted to center the orbit between the aperture limits. Then, by repeating the process successively with each corresponding set of correction coils

about the ring, the computer optimizes the beam intensity. Although this system has actually been used, we find that manual tuning of even a very small number of correction coils, less than five, makes a very good orbit.

Targets and photon beams

A magnetic distortion of the orbit will deviate electrons to a target. Near the peak of the magnetic cycle, when the electrons are near full energy, a large current pulse is applied in series to two coils wound about the pole tips of two suitably chosen magnets. These coils are connected noninductively with respect to the main excitation circuit and they provide fields that produce a well localized radial bump in the beam, either for producing an external bremsstrahlung beam or for studying electron interactions in the target itself. For interaction studies the target is in the long straight section in the middle of the experimental hall to ensure good access to the interaction area.

The bremsstrahlung beam emerges through a special channel in the side of the appropriate magnet, and it then passes along the flare of the experimental hall to apparatus set up on the floor. In figure 6 we show the beam lines as they now exist, together with a schematic diagram of the various experimental arrangements. Currently we have four external photon beam lines, which pass through collimators and broom magnets (not shown in figure 6) as they traverse the west flare. Thus all the pretreatment necessary to define and clean the beam is done before it passes through the lead and concrete shielding wall into the main experimental area.

The size of the building determines the general scale of the operation. Our experimental hall measures 30 × 30 meters, and it accommodates six experiments simultaneously with some margin. Of course these are only "first-generation" experiments and we expect that as larger experiments come on to the floor it will become more crowded. The site will accommodate future expansion.

We hope that we can increase the synchrotron duty cycle, which is currently limited by the energy spread that we can tolerate. With sinusoidal magnet excitation a 1% energy spread yields a duty cycle of 7%. In principle the excitation system is sufficiently flexible to let us install a "flat-top" system that would clamp the magnet at peak field and permit a duty cycle as great as 50%.

Although the design energy for the accelerator is 10 GeV, many of the components, including the main guide field, would permit operation at an energy higher than 15 GeV. We think we can increase the accelerating voltage either by a brute-force approach or with superconducting cavities to obtain higher peak energy for the accelerator.

Work is now in progress to produce an external beam with slow extraction. We hope to have it operating in 1969.

EXPERIMENTAL PROGRAM

For some twenty years experiments done with electron accelerators have made decisive contributions to our understanding of elementary particles. Recall, for example, the discovery of the π^0 meson in the elegant experiments of J. Steinberger, W. K. H. Panofsky, and J. Steller[3] at Berkeley, the fundamental work of Robert Hofstadter at Stanford on elastic electron scattering, so fittingly extended to the multi-GeV range by recent work with the Stanford linear accelerator,[4] the work at Cornell and Cal Tech that led to the discovery of the first nucleon isobars and played so important a role in determining their quantum numbers,[5] the various experiments extending the domain of validity of quantum electrodynamics (QED) culminating in the brilliant work at the German electron synchrotron (DESY)[6] and the experiments at the Cambridge electron accelerator and DESY on the photoproduction of vector mesons, a uniquely powerful way to investigate their strong interactions.[7,8]

With this rich tradition in mind we began our experimental program impatiently almost before the last magnet was in place and months before the building was finished.

Tests of QED

Electromagnetic interactions are remarkably well described by the theory

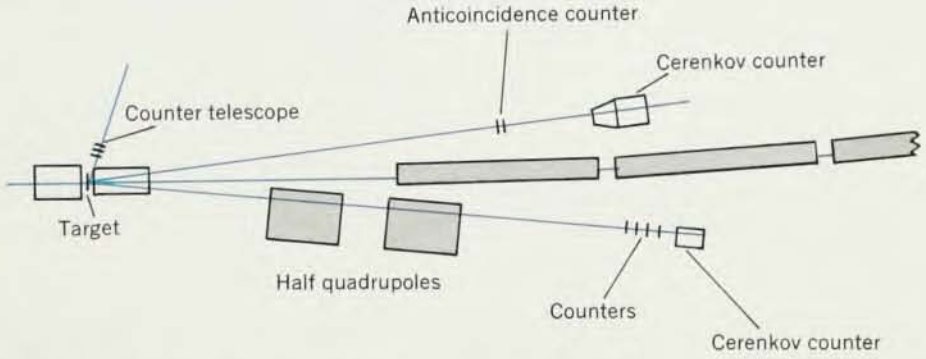

WIDE-ANGLE BREMSSTRAHLUNG measurements. Internal electron beam strikes a target in one of the straight sections; scattered electrons pass through the two half quadrupoles and the momentum-defining counters into the lead-glass total-absorption Cerenkov counter. The scattered photon is detected in the other Cerenkov counter. The well known elastic-scattering cross section from hydrogen serves to calibrate the electron arm of the apparatus. Counter telescope near the target detects the recoil proton in the elastic scattering. —FIG. 8

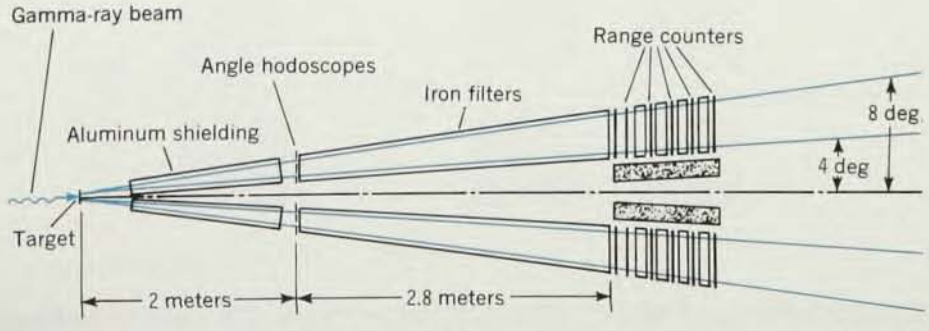

MUON-PAIR PRODUCTION experimental arrangement. Muon pairs produced in the target traverse the aluminum shielding in which strongly interacting particles are absorbed. Muon production angles are measured in the angle hodoscopes; their range determines momentum, and their invariant mass can then be calculated from their energies and the angle between them. —FIG. 9

of quantum electrodynamics (QED). For example, this theory calculates the Lamb shift in hydrogen with an accuracy of better than 1 part in 10^4. However, atomic energy levels are rather insensitive to the short-distance behavior of the electromagnetic interaction. High-energy electrons and photons are very useful for investigating this short-distance behavior–for example, the recent experiment at DESY[6] on wide-angle electron-pair production showed that QED remains valid down to distances of perhaps 10^{-14} cm. Clearly we should continue these investigations to smaller distances.

To this end we started two experiments, wide-angle bremsstrahlung and muon-pair production, some time ago; a third, wide-angle electron-pair production, will begin soon. The first two are through the tune-up stage and are now accumulating data. Figure 7 shows three of the Feynman diagrams involved in these processes. The invariant mass of the two light particles in the final state offers a convenient way to describe the severity of the test to QED. For example the major contribution to electron-pair production comes from invariant masses of the electron pair of about 1 MeV where QED has been investigated in great detail. These experiments will investigate the mass region from 500–1500 MeV. In this range a major contribution to the counting rate in pair experiments comes from leptonic decays of the vector meson, which somewhat complicate the purely QED aspects while at the same time enriching the experiment. The bremsstrahlung experiment does not face this complication and may, therefore, be the most direct test of QED in the same mass range.

So far QED has survived the most determined assaults. A possible crack in the dike has been recently reported from CERN–a tantalizing two or three standard-deviation discrepancy in the anomalous moment of the muon.[9]

Figures 8 and 9 show the wide-angle bremsstrahlung and muon-pair experimental arrangements.

Vector-meson family

The existence of the vector-meson family was predicted to account for the electromagnetic form factors of the nucleus. Vector-meson electromagnetic and strong interactions are of great interest to any theory of elementary particles and photoproduction offers us a very powerful tool for investigating these interactions. For example the total cross section for rho-meson–nucleon scattering has been determined with an accuracy of perhaps 10% by a study of ρ^0 photoproduction from complex nuclei–a rather remarkable achievement considering that the mean life of a rho-meson is approximately 10^{-23} sec.

We have measured ρ^0 photoproduction from 4 to 9 GeV with various targets, including hydrogen and deuterium. Previous measurements have shown that the ρ^0 is photoproduced in diffraction-like processes.[8] A particularly attractive mode that allows for diffraction production is the vector-dominance model, according to which the photon interacts with hadrons only by first changing to a vector meson.[10] Figure 10 shows the important Feynman diagram for ρ^0 production from hydrogen in this theory. Similar diagrams apply to phi and omega production. This theory yields the rho-nucleon total cross section and the strength of direct gamma-rho coupling from measurements on various nuclei.[11] Recent measurements at this laboratory subject this model to more detailed and quantitative tests than before; they confirm the main features of earlier measurements but disagree with some of the quantitative conclusions. Figure 11 shows the apparatus we used for these measurements. The same apparatus, suitably modified, will study phi-production, wide-angle electron pairs, and leptonic decays of vector mesons.

We are preparing an extension to these measurements with the polarized beam obtained from radiation from a diamond crystal.[12] Measurements with polarized photons offer a very powerful tool for sorting out the polarization states of the rho meson, information of great usefulness for an understanding of the basic phenomena involved. Clearly, polarized photon beams can be useful in many different experiments and we expect they will play an important role in future experiments.

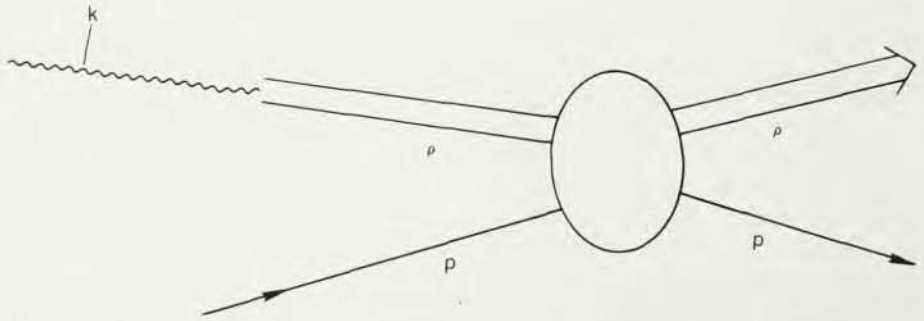

FEYNMAN DIAGRAM for the dominant process in $\gamma p \rightarrow \rho p$ according to the vector-dominance theory. Similar diagrams apply to nuclei other than hydrogen. Strength of the direct γ–ρ coupling is measured by $em_\rho^2/2\gamma_\rho$. **—FIG. 10**

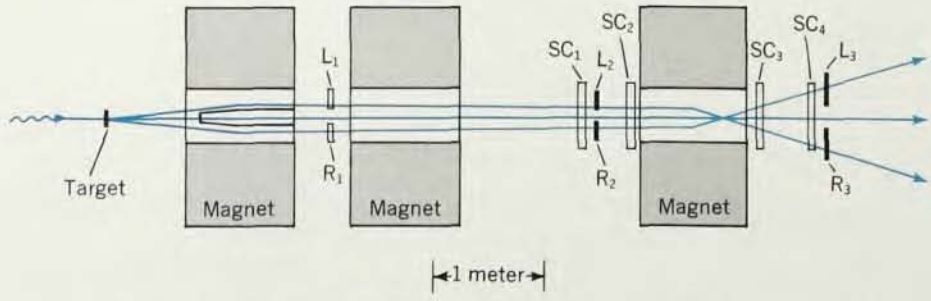

EXPERIMENTAL ARRANGEMENT for ρ^0 measurements. Rho mesons produced from photons in the target decay into positive and negative pions. A six-fold coincidence in the scintillation counters triggers four optical spark chambers, which determine the pion trajectory. In this way the invariant mass, energy and angle of the pion pair is determined. Detection system rotates through 100 milliradians in the vertical plane and can also be rotated about a vertical axis. Center magnet of the three shown will be used in later experiments. **—FIG. 11**

Omega production

Rochester and Cornell in collaboration are studying ω^0 photoproduction using the apparatus shown in figure 12. Information on ω^0 photoproduction is

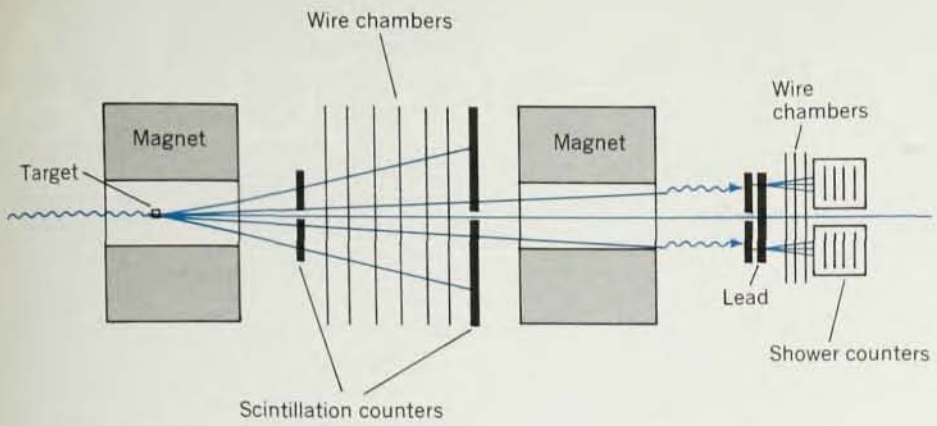

OMEGA-PRODUCTION EXPERIMENT. ω^0 **mesons are produced when the gamma-ray beam passes through the target in a uniform magnetic field; pions from the** ω^0 **decay are detected in the apparatus behind the magnet. Positive and negative pions pass through a pair of scintillation counters with wire spark chambers between them. Decay photons from the neutral pions pass through a second magnet that sweeps out charged particles. They are then converted in a lead radiator and detected in wire chambers and shower counters. The experiment is "on line" to an IBM 1800 computer where the kinematics of the event are reconstructed.** —FIG. 12

much less extensive than for the ρ^0, partly because the cross section is smaller and partly because the three-body decay makes detection more difficult. Data obtained from hydrogen bubble chambers at energies of 2–6 GeV indicate that omega production involves both single pion exchange and diffraction dissociation.[8] If this explanation is true the diffraction dissociation will dominate at higher energies and measurements made on heavy nuclei will yield the omega–nucleon cross section and omega–gamma coupling constant, as in the case of the rho meson.

Pions and kaons

Figure 13 shows the arrangement of an experiment to measure π^+ and K^+ produced near 180 deg in the center-of-mass coördinate system in these three reactions

$$\gamma p \rightarrow \pi^+ n \qquad (1)$$

$$\gamma p \rightarrow K^+ \Sigma^0 \qquad (2)$$

$$\gamma p \rightarrow K^+ \Lambda^0 \qquad (3)$$

Meson photoproduction at backward angles is particularly interesting as it offers a very sensitive way to investigate processes in which a baryon is exchanged. Reasonably extensive measurements have been made on the energy dependence of reaction 1 from 600 MeV to 3 GeV.[13] These measurements show the same sort of rich structure characteristic of elastic scattering of pions in the backward direction, structure presumably associated with the formation of nucleon isobars. Information above 3 GeV is insufficient to determine whether this structure continues at higher energy or not. Information on reactions 2 and 3 is rather meager at all energies.

Recent measurements at SLAC[14] show that the angular distribution of reaction 1 near 180 deg is rather different from that obtained in the elastic scattering of pions, a fact that may be difficult to reconcile with the popular belief that all these processes are dominated by baryon exchange. More experimental information should be very useful in the interpretation of these results.

Preliminary results show that the experiment can easily be run at a beam intensity corresponding to a hundred counts per hour of pions or kaons produced by 10-GeV photons. We expect to cover the energy range from 3 to 10 GeV rather carefully.

K^0 mesons are detected in the apparatus shown in figure 14. We detect long lived K^0 mesons, produced at a fixed laboratory angle, 20 meters from the target by regeneration of short lived K^0 mesons that decay in the apparatus. The spectrum of these K^0 mesons tells us something about the mechanism by which they are photoproduced. In particular, the spectrum can be analyzed for those K^0 mesons that arise from phi-meson decay and the phi-meson cross section thereby determined.

Next year and later

We hope to investigate the neutron form factor by detecting the scattered electron and recoil proton in coincidence, in the manner of P. C. Stein and others.[15] This technique provides the least ambiguous method for determining neutron form factors, a task complicated by the absence of free neutrons.

Inelastic electron scattering with detection of the scattered electron and

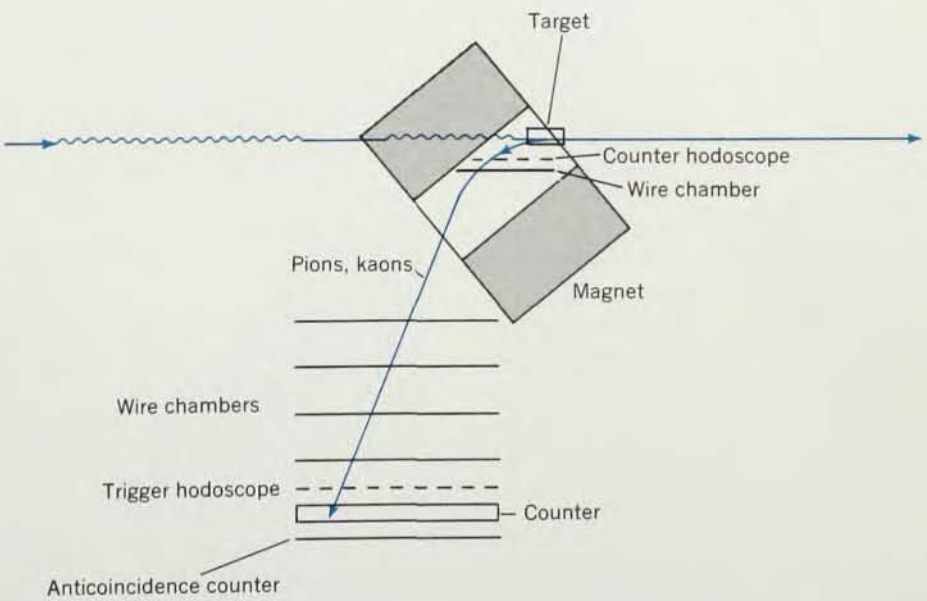

BACKWARD PION AND KAON MEASUREMENTS. π^+ **and** K^+ **mesons produced in the hydrogen target at laboratory angles close to 180 deg pass through the counter hodoscope and wire chamber, are bent through about 90 deg in the magnet and then traverse more wire chambers, another hodoscope and a counter in which they are stopped. Protons, pions and kaons are distinguished by time of flight, pulse height in the stopping counter, and range. The wire chambers can determine momentum to about 0.1%. This experiment is "on line" to an IBM 1800 computer.** —FIG. 13

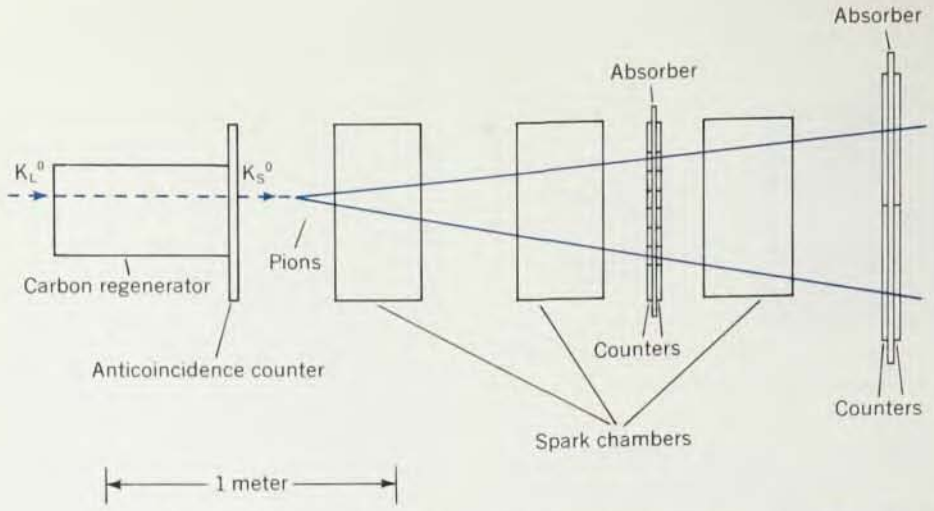

DETECTION OF K⁰ MESONS. Long lived K⁰ mesons from a target about 20 meters upstream from the detector pass through the carbon regenerator from which about 0.3% emerge as short lived K⁰ mesons. Eightfold coincidence in the scintillation-counter hodoscopes detects pions from K_S^0 decay and triggers the spark chambers. The direction of the initial kaon together with the decay directions of the pions, as determined in the spark chambers, defines the momentum of incident K_L^0. —FIG. 14

another particle (pion, proton, rho meson, etc) in coincidence, could also be investigated here. This work would be similar to the pioneer work of K. Berkelman on the pion form factor and the γNN^* (1238) form factor.[16] Inelastic electron scattering offers a very rich field and is likely to be an important part of our experimental program for some years.

Later we could investigate the photoproduction of strange particles (for example $\gamma p \rightarrow Y^*K^+$) in which the K^+ is detected in coincidence with one of the Y* decay products. Experiments at Cornell and by a Yale group at Cambridge detect only the K^+ in a "missing-mass" type of experiment that suffers from a large nonresonant background. Quantitative information is therefore hard to get; detection of the Y* through one of the decay products will greatly reduce this nonresonant background. Quantitative information on this kind of reaction will allow us to test a number of SU_3 and quark-model predictions.

Collaboration and comparisons

Currently physicists from four outside institutions are collaborating with Cornell staff in the experimental program. As the program matures and as more equipment becomes available we expect outside users to increase in number and to work in independent groups. Our understanding with the National Science Foundation, our funding agency, is that machine time shall be available to qualified outside users in an amount comparable to that allocated to our own staff. With this understanding in mind, we encourage proposals from outside groups and will accommodate them to the extent to which our facilities permit and their proposals qualify.

This brief description of our experimental program makes clear the heavy debt we owe to other electron accelerators. Many of our experiments are extensions into a new energy region of work done at CEA and DESY, where the experimenters, of course, owe a similar debt to their predecessors.

Comparison of our experimental program with that of SLAC reveals that though they overlap in some areas, they tend, on the whole, to complement each other, largely as a result of the complementary characteristics of the two accelerators. The longer duty cycle of the synchrotron makes it easier to do experiments in which two or more particles are detected in coincidence—a characteristic of most of the experiments we describe here. The higher intensity of the linear accelerator makes possible the measurements of very small cross sections (for example, the recent beautiful proton form-factor measurements) and the production of particle beams. These differences in accelerator characteristics affect both the choice and the style of experiments in the two laboratories.

No doubt electron accelerators will continue their important role in elementary-particle physics, a role that we at Cornell are looking forward to sharing.

References

1. R. R. Wilson, *The 10 to 20 GeV Cornell Synchrotron*, CS-33, Laboratory of Nuclear Studies, Cornell Univ., Ithaca, N.Y. (1967).
2. T. L. Collins, *Long Straight Sections for A. G. Synchrotrons*, CEA-86, Cambridge Electron Accelerator, Cambridge, Mass. (1961).
3. J. Steinberger, W. K. H. Panofsky, J. Steller, Phys. Rev. **78**, 802 (1950).
4. Robert Hofstadter, *Nuclear and Nucleon Structure*, W. A. Benjamin, Inc., N.Y. (1963).
   R. E. Taylor, in *Proceedings of the International Symposium on Electron and Photon Interactions at High Energy*, Stanford Linear Accelerator Center, Stanford University, 5–9 Sept. 1967, page 78. Available from National Bureau of Standards, Springfield, Va.
5. R. L. Walker, D. C. Oakley, A. V. Tollestrup, Phys. Rev. **89**, 1301 (1953); M. Heinberg *et al*, Phys. Rev. **110**, 1210 (1958); R. R. Wilson, Phys Rev. **110**, 1212 (1958); F. D. Dixon, R. L. Walker, Phys. Rev. Letters **1**, 142 (1958); P. C. Stein, Phys. Rev. Letters **2**, 473 (1959).
6. J. G. Asbury *et al*, Phys. Rev. Letters **18**, 65 (1967).
7. L. J. Lanzerotti *et al*, Phys. Rev. Letters **15**, 210 (1965).
   J. G. Asbury *et al*, Phys. Rev. Letters **19**, 865 (1967).
8. F. M. Pipkin, 1967 Stanford conference on electron and photon interactions (see ref. 4). This paper provides a very useful review of experimental and theoretical work on vector-meson photoproduction.
9. J. M. Farley, American Physical Society meeting, April 1968, Washington, D.C.
10. N. M. Kroll, T. D. Lee, B. Zumino, Phys. Rev. **157**, 1376 (1967).
11. J. G. Asbury *et al*, Phys. Rev. Letters **20**, 227 (1968).
12. G. Barbiellini *et al*, Phys. Rev. Letters **8**, 454 (1962).
13. R. A. Alveraz, private communication.
14. B. Richter, 1967 Stanford conference on electron and photon interactions (see ref. 4). This reference contains a rather comprehensive review of high-energy meson photoproduction.
15. P. C. Stein *et al*, Phys. Rev. Letters **16**, 592 (1966).
16. C. W. Akerlof *et al*, Phys. Rev. **163**, 1482 (1967).
17. W. Blanpied *et al*, Phys. Rev. Letters **14**, 741 (1965); N. B. Mistry *et al*, Phys. Letters **24B**, (1967).
18. Joseph Ballam, "SLAC: The Program," Physics Today, **20**, No. 4, (1967) page 43. □